Preprint version of:
A. Suarez, H. Romero, R. Salmoral, J. A. Acosta, J. Zambrano, A. Ollero, "Experimental Evaluation of Aerial Manipulation Robot for the Installation of Clip Type Bird Diverters: Outdoor Flight Tests" in 2021 Aerial Robotic Systems Physically Interacting with the Environment (AIRPHARO), 2021, pp. 1-7.

Experimental Evaluation of Aerial Manipulation Robot for the Installation of Clip Type Bird Diverters: Outdoor Flight Tests

Alejandro Suarez[1], Honorio Romero[1], Rafael Salmoral[1], José Alberto Acosta[2], Jesús Zambrano[2], and Anibal Ollero[1]

***Abstract*— This paper presents an aerial manipulation robot intended to conduct the installation of clip-type bird diverters on power lines, consisting of a multirotor platform equipped with a high force linear actuator and a clamp mechanism that holds the device until it is exerted on the cable. The installation mechanism has been specifically designed for a particular model of bird flight diverter that is extensively employed on the Spanish power grid. The paper analyzes the risks involved in this operation and describes the approach followed in the validation of the aerial robot, from the installation in indoor testbed, to representative outdoor scenario, and preliminary flight tests on a 15 kV power line to identify possible malfunctions on the platform due to the electrostatic discharge.**

***Index Terms* – Aerial Systems: Applications.**

I. Introduction

The installation of bird flight diverters on the power lines as the ones depicted in Figure 1 is a relevant activity conducted by the companies in charge of their maintenance, which is intended to protect the bird species from the collision and/or electrocution with the cables. These devices, installed usually each 5 or 15 meters on the highest line, act as markers so birds can detect the lines and avoid the impact when flying. The features of these devices in terms of color, size, or shape may vary according to the regulation of each particular region or country. Two types of bird flight diverters can be found: clip-type [1][2] or helical type [3][4]. The main difficulty in their installation is the access to the power line, whose altitude may vary between 15 and 50 meters for medium and high voltage power grids. Not only that, but the operation is conducted on live power lines to avoid the interruption of the service, with voltages between few kilovolts, up to several hundreds of kilo volts. This makes this operation particularly risky for human workers, who must perform the task from manned helicopters, perching from the line, or using elevating work platforms [5]. Thus, considering the vast extension of the power grid, which comprises tens of thousands of kilometers on a single country, it is highly desirable to consider new robotic technologies that contribute to reduce the time, cost and risk in the realization of this kind of operations.

In this sense, the AERIAL-CORE project proposes the use of aerial robots for the inspection and maintenance of power lines, motivated by the ability of this kind of platforms to reach quickly and operate in high altitude workspaces [6]. Aerial manipulation robots [7][8][9] extend the functionalities and capabilities of unmanned aerial vehicles (UAVs) like multi-rotors and helicopters with the integration of end effectors [10] [11][12] or robotic arms [13][14][15] that allow the realization of manipulation tasks on flight, while perching [16][17], or once the platform has landed on the workspace [18].

The use of multirotor platforms for power line inspection and maintenance has been already proposed and documented in some works. Reference [19] is focused on the landing on the power line using a vision system and a LiDAR, whereas [20] presents a pneumatic-mechanical system designed to install sensor devices on the power line. In our previous work [21] we analyzed the effect of the electrostatic discharge (ESD) raised when an aerial manipulation robot interacts with a high voltage power line, relying on related literature [22][23][24].

Figure 1. Clip-type bird flight diverters installed on power lines (left). Aerial manipulator with linear actuator performing the installation of the device on a section of power line in a representative outdoor scenario (right).

The main contribution of this paper is the experimental evaluation of a prototype of aerial manipulation robot intended to conduct the installation of clip-type bird diverters on power lines. The robot consists of a quadrotor platform equipped with a high force linear actuator and a clamp mechanism that holds the device until this is exerted on the cable. The paper covers the installation procedure and the risk assessment taking into account diverse factors identified during the realization of the experiments. The developed prototype is validated in a representative outdoor scenario, including preliminary flight tests on a real 15 kV power line.

The rest of the paper is organized as follows. Section II describes the installation procedure and possible operational risks. Section III presents the aerial manipulation robot and the validation scenarios. Section IV covers the modelling and control of the aerial robot. Experimental results are shown in Section V, whereas Section VI summarizes the conclusions.

[1] GRVC Robotics Labs, University of Seville (https://grvc.us.es).
E-mail: asuarezfm@us.es, aollero@us.es, rafaslasla@gmail.com, hromero_r@hotmail.com

[2] ENEL Specialized Maintenance. E-mail: josealberto.acosta@enel.com, jesus.zambrano@enel.com

II. Problem Statement

A. Installation Procedure

The purpose of this work is the development of an aerial robot capable to perform the installation of the clip-type bird flight diverter shown in Figure 1 and whose specifications can be found in [1]. The installation procedure simply consists of placing the device groove over the cable and apply a pushing force until it is completely exerted. The rubber body (red) ensures that the device, once installed, does not slide on the cable due to the wind or vibrations. Although the weight of the device (300 grams) is affordable for conventional multirotors, the relatively high force (around 200 N) required to perform the installation cannot be supported by most platforms. Note that these devices are traditionally installed by human workers. Thus, the installation mechanism should grab the line to form a closed kinematic chain to support the reaction force exerted on the device, similarly to what human workers do with their fingers. In this way the aerial platform is partially isolated from the force.

The proposed installation procedure with the aerial robot involves two persons, the drone pilot and the device operator, and consists of five phases:

1. The device is loaded into the installation mechanism of the aerial robot by the device operator.
2. The platform, controlled from the ground control station by the pilot, takes-off and approaches from above to the power line.
3. The platform approaches slowly to the power line until the installation mechanism is in the correct position.
4. The device is installed while the platform hovers.
5. Once the device is installed, the platform flies up and goes back to the ground control station.

The main challenge here is associated to phases 3 – 4, since the aerial platform should be controlled with high positioning accuracy in an outdoor environment. The experiments carried out as part of this work indicate that the human pilot loses the depth perception when the aerial platform is flying close to the power line (at 15 m height in the experiments). Therefore, the aerial robot should be equipped with a vision system to detect and localize the power line once it is close enough, so the operation is executed autonomously and in a more reliable way [19][20].

B. Risk Analysis

The proposed solution for installing bird flight diverters on power lines with aerial robots presents some risk factors that have to be carefully considered during the development and validation of the system:

- Electromagnetic interference on the aerial platform. The proximity of the robot to the high voltage power line, and particularly during the installation phase, may affect the IMU (inertial measurement unit), autopilot, or electronic speed controllers, with the consequent risk of collision or crash [21].
- Entrapment of the aerial robot with the power line. In case of collision with the cables, fault of the controller, or perturbation during the installation of the device, it is preferable that the platform falls down to the ground than it is caught in the cables, as retrieving the robot from the power line would require heavy vehicles and involves a certain risk for the workers.
- Interaction with birds. The aerial manipulation operation should not disturb the surrounding birds, for example in nests or when these are perched on the power lines, as this involves a certain risk of collision.
- Wind gusts and interaction forces. During the installation operation, the motion of the aerial platform is constrained by the power line, so the position deviations caused by unexpected wind gusts may destabilize the platform and cause the crash or entrapment.

The first two factors must be considered during the design and development of the aerial robot, whereas the other two are associated to the realization of the operation.

C. Operational Constraints

The IEEE Guide for Maintenance Methods on Energized Power Lines [5] defines the minimum air insulation distance (MAID) as "the shortest distance in air between an energized electrical apparatus and/or a line worker's body at different potential." This distance, which depends on the voltage of the power line, must be respected to prevent the spark between the power line and the operator/robot, with the consequent injury, damage, or breakdown of the power grid. For the 15 kV power line considered in this work, the MAID is 5 cm. For a 72 kV power line, the MAID is 28 cm. In practice, this implies that the aerial robot must not fly between any pair of phases of the power line. The aerial platform should approach from above, from below, or from one side of a single phase. If the distance between the phases and robot is under the MAID, the aerial platform may act as electrode at floating potential, facilitating the rise of the electric arc.

III. Developed Prototype

A. Device Installation Robot

The aerial robot developed for the installation of clip-type bird diverters is shown in Figure 2. It consists of a Proskytec LRM multirotor, whose features are indicated in Table 1, and the installation mechanism. This is built with a Firgelli linear actuator (90 kg force, 10 cm stroke) and a customized clamp mechanism with a 3D printed claw and an aluminum frame structure that holds the device to be installed [25]. A M-shaped steel rod structure is placed at both sides of the claw in order to facilitate the alignment with the power line when the aerial robot approaches for the installation phase. The mechanism is attached to the multirotor base with a passive joint, providing a certain level of accommodation to position and orientation deviations. The battery and control electronics of the actuator are placed next to it, being electrically insulated to avoid the propagation of the electrostatic discharge [21] to the multirotor control system, which also facilitates undocking the system. The electronics consists of an H-bridge and a microcontroller board that control the stroke position of the linear actuator, which is activated by the device operator from the ground control station through a radio transmitter.

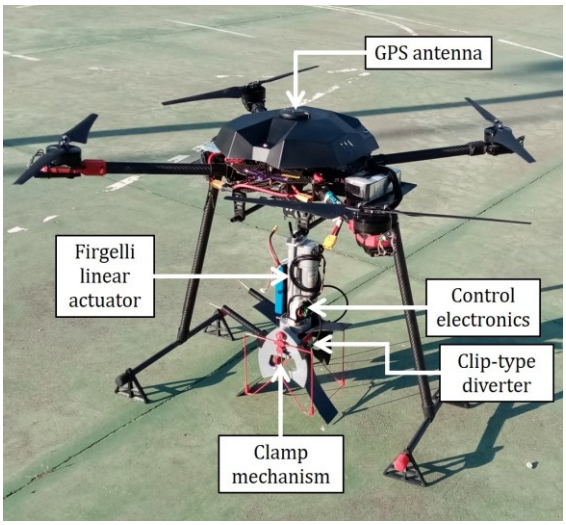

Figure 2. Aerial manipulation robot with installation mechanism.

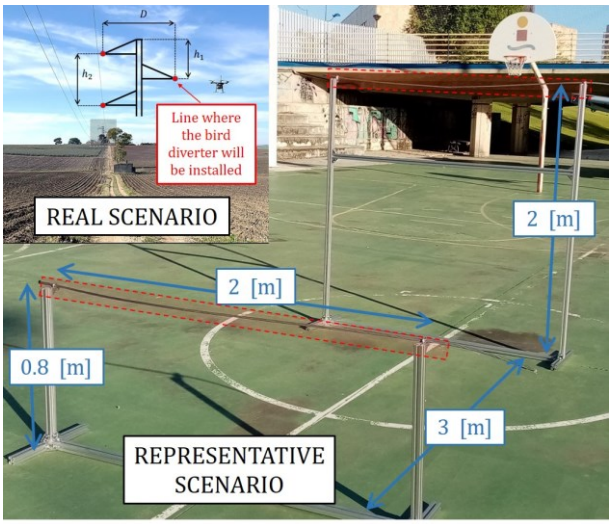

Figure 3. Representative outdoor scenario that replicates the real power line.

Table 1. Main features of the aerial platform.

Weight [kg]	6
MTOW [kg]	9.5
Max. flight time [min]	45
Propellers (inches)	21 × 7
Autopilot	Pixhawk 2
Firmware	Arducopter
LiPo Battery (mAh)	12S, 7000
Brushless motors	DJI E2000
Max. ascend. speed (m/s)	1.5
Max. cruise speed (m/s)	3

Table 2. Parameters of interest of the power line scenario.

Parameter	Description	Value
D	Horizontal distance between phases	1.5 [m]
H	Phase-to-ground distance (mid phase)	12 [m]
h_1, h_2	Vertical distance between phases	1.2 [m]
S	Cable section	9 [mm]

The time since the operator triggers the linear actuator until the device is installed on the cable is around 12 seconds, given by the required stroke (5 cm) and linear speed of the actuator (0.4 cm/s). During the installation phase, the aerial platform is physically attached to the power line by the claw mechanism, so the position controller must be accurate enough to avoid that undesired deviations destabilize the multirotor. Once the clip-type diverter is installed, the claws are opened and the robot is released.

B. *Outdoor Test-bench*

In order to facilitate the realization of installation tests with the aerial robot in a controlled outdoor environment, a power line test-bench has been built using Rexroth bars and sections of real cable. The test-bench, depicted in Figure 3, replicates the relative separation distances between the phases of a real power line, as indicated in Table 2. This is a single circuit transmission line in which one of the phases is separated from the other two. This configuration results particularly suitable for the preliminary tests at it reduces the risk of entrapment in case of fault of the aerial platform.

The test-bench is placed at a 25 × 25 m size outdoor area within the School of Engineers of Seville, which is covered by a safety net, 10 m height. This allows to evaluate the accuracy of the aerial robot with GPS (Global Positioning System) and RTK (Real-Time Kinematics) GPS.

IV. Modeling and Control

This section derives the kinematic and dynamic models of the aerial manipulation robot performing the installation on flight of the bird flight diverter, describing later the control scheme implemented by the autopilot. Since the installation mechanism is attached to the multirotor base by a passive joint (spherical) that allows the free rotation in the three angles, the free-flying dynamics of the aerial robot can be assimilated to the cable suspended configuration as described in [26][27], whereas the model associated to the physical interaction can be approached as done in [28][29].

A. *Kinematics and Dynamics*

Two reference frames are defined in the proposed aerial manipulation operation, as represented in Figure 4: the Earth fixed frame $\{\boldsymbol{E}\} = \{\boldsymbol{X_E Y_E Z_E}\}$, whose origin corresponds typically with the take-off position, and the multirotor base frame $\{\boldsymbol{B}\} = \{\boldsymbol{X_B Y_B Z_B}\}$, located at its center of mass. The position and orientation of the aerial platform with respect to the inertial frame is denoted by ${}^{\boldsymbol{E}}\boldsymbol{r_B} = [x_B, y_B, z_B]$ and $\boldsymbol{\eta_B} = [\phi, \theta, \psi]$, respectively, where ϕ, θ, and ψ are the roll, pitch and yaw angles. The installation mechanism will be modelled as a rigid link of length L, attached on one side to the center of mass of the multirotor base by a passive spherical joint that can rotate in the three angles (roll, pitch, and yaw), and on the other side it is attached to the power line at the installation

point, ${}^{E}\boldsymbol{r}_{IP}$. This can be expressed in the multirotor frame $\{\boldsymbol{B}\}$ applying the following transformation:

$$\begin{bmatrix} {}^{B}\boldsymbol{r}_{IP} \\ 1 \end{bmatrix} = {}^{B}\boldsymbol{T}_{E}(\phi, \theta, \psi, {}^{E}\boldsymbol{r}_{B}) \begin{bmatrix} {}^{E}\boldsymbol{r}_{IP} \\ 1 \end{bmatrix} \quad (1)$$

where ${}^{B}\boldsymbol{T}_{E} \in \Re^{4\times4}$ is the homogeneous transformation matrix between $\{\boldsymbol{E}\}$ and $\{\boldsymbol{B}\}$. Although the device installation mechanism provides a certain degree of accommodation to position deviations in the multirotor, it is assumed that, during the installation phase, the following constraint arises:

$$\left\| {}^{E}\boldsymbol{r}_{IP} - {}^{E}\boldsymbol{r}_{B} \right\| = L \quad (2)$$

The multirotor platform will be affected by three types of forces as depicted in Figure 4: (1) the thrust $T_i, i = \{1, 2, 3, 4\}$, generated by the propellers, (2) the gravity, and (3) the external force due to the interaction with the power line:

$$\boldsymbol{F}_{ext} = F_{ext}\boldsymbol{n}_{ext} \quad ; \quad \boldsymbol{n}_{ext} = \frac{{}^{E}\boldsymbol{r}_{IP} - {}^{E}\boldsymbol{r}_{B}}{\left\| {}^{E}\boldsymbol{r}_{IP} - {}^{E}\boldsymbol{r}_{B} \right\|} \quad (3)$$

where F_{ext} is the magnitude of the force, and $\boldsymbol{n}_{ext}$ is the unit vector that determines the direction of application on the aerial base. The dynamic model of the aerial manipulation robot can be derived from the Lagrangian and the generalized equation of the forces and torques [26][27][29]. The vector of generalized coordinates $\boldsymbol{q} = [\, {}^{E}\boldsymbol{r}_{B} \quad {}^{E}\boldsymbol{\eta}_{B} \,] \in \Re^{6}$ comprises the position and orientation of the platform, so the equations of motion can be expressed in the usual matrix form:

$$\boldsymbol{M}(\boldsymbol{q})\ddot{\boldsymbol{q}} + \boldsymbol{C}(\boldsymbol{q}, \dot{\boldsymbol{q}}) + \boldsymbol{G}(\boldsymbol{q}) = \boldsymbol{\Gamma} + \boldsymbol{\Gamma}_{ext} \quad (4)$$

where $\boldsymbol{M} \in \Re^{6\times6}$ is the generalized inertia matrix, $\boldsymbol{C} \in \Re^{6}$ represents the centrifugal and Coriolis terms, whereas $\mathbf{G} \in \Re^{6}$ includes the gravity component. Finally, vectors $\boldsymbol{\Gamma}$ and $\boldsymbol{\Gamma}_{\text{ext}} = [\mathbf{F}_{\text{ext}} \quad 0]$ comprise the wrenches generated by the propellers and the external force. Note that the force exerted by the linear actuator is not transmitted to the multirotor due to the clamp mechanism, and the torque is zero due to the passive joint.

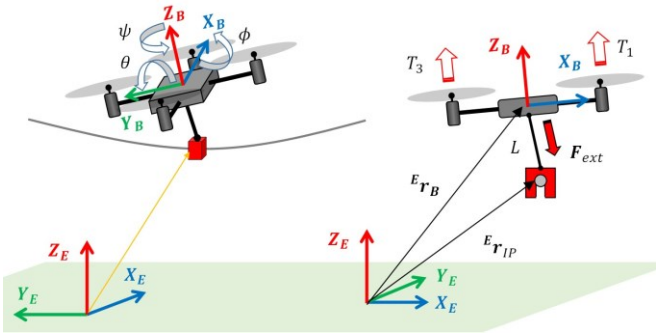

Figure 4. Kinematic model of the aerial manipulation robot installing the clip-type bird flight diverter. 3D view (left) and 2D view on the $\boldsymbol{X_B Z_B}$ axes (right).

B. Control Scheme

The Arducopter firmware executed on the Pixhawk auto-pilot implements the usual PID-cascade controller as shown in Figure 5 [30][31]. The diagram represents only the pitch angle controller along with the vertical speed control since the scheme for the roll and yaw angles is the same. The human pilot provides through the radio controller the XYZ velocity and yaw rate references taken as input by the autopilot. On a first stage, a PID velocity controller transforms the velocity error into a reference in the pitch angle:

$$\theta_{ref} = PID(v_e^x) \quad ; \quad v_e^x = v_{ref}^x - v^x \quad (5)$$

where v^x, v_{ref}^x and v_e^x are the measured, reference, and error velocity in the X-axis, respectively (the Y-axis velocity is controlled through the roll angle), whereas $PID(\cdot)$ denotes the PID control function defined as:

$$u = PID(e) = K_p\left(e + \frac{K_i}{T}\int edt + k_d\dot{e}\right) \quad (6)$$

In the second stage, a proportional controller converts the attitude error $\theta_e = \theta_{ref} - \theta$ into a reference angular rate $\dot{\theta}_{ref}$. Finally, the PID rate controller takes as input the angular rate error giving as output the control signal for the pitch angle:

$$U_2 = PID(\dot{\theta}_e) \quad ; \quad \dot{\theta}_e = \dot{\theta}_{ref} - \dot{\theta} \quad (7)$$

This scheme is also applied for the roll and yaw angles, ϕ and ψ, whose corresponding outputs are U_1 and U_3. The multirotor attitude, angular rate, and velocity are estimated by an Extended Kalman Filter (EKF) that integrates the measures from the inertial measurement unit (IMU) and GPS sensor. On the other hand, the altitude of the platform is controlled by the human pilot through the Z-axis velocity reference, v_{ref}^z, taken as input along with the estimated velocity by the PID climbing rate controller that gives as output the thrust signal U_4. The motor mixer block converts the control signals of the roll (U_1), pitch (U_2), yaw (U_3), and thrust (U_4) into the PWM (pulse width modulation) signals used by the electronic speed controllers (ESC) to produce the required thrust in the four rotors.

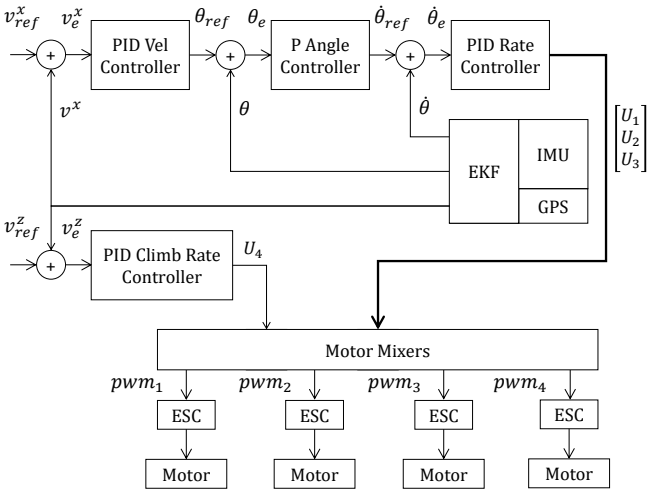

Figure 5. PID cascade controller of the multirotor for the pitch angle and climbing rate (Z-axis).

V. Experimental Results

A. Installation of Clip-Type Bird Diverter

The performance of the aerial installation robot has been evaluated in the outdoor test-bench presented in previous sub-section. A sequence of images taken from the recorded video [32] corresponding to two different experiments is depicted in Figure 6. The evolution of the multirotor position, velocity, and attitude is represented in Figure 7, whereas Figure 8 shows the battery voltage and current. This data is useful to identify situations in which the aerial platform is physically interacting with the power line. The aerial platform was controlled in GPS position mode by a human pilot. Before the platform takes-off, the operator puts the device on the clamp mechanism. The installation procedure is the same as described in Section II-A. The main difficulty in the realization of the experiments is on the accurate position control during the installation phase since the human pilot has to compensate manually deviations due to GPS errors, small wind gusts, and also the reaction wrenches exerted by the linear actuator over the multirotor base. As it can be seen in Figure 7, the installation phase occurs between t = 46 and t = 64 s. The coupling of the platform with the power line corresponds to the peak around t = 48 s. It is interesting to observe the current drop at the same instant in Figure 8, which indicates that the platform is momentarily resting on the power line, supported by the installation device. It was observed that the propellers tend to reduce momentarily but significantly the thrust when the platform tends to rest on the linear actuator while it is grabbed to the cable, resulting in a certain loss of the attitude control. It is also necessary to remark that, unlike the real power line, in which a single cable may weight tens or hundreds of kilograms, being almost completely rigid due to the tension created by its own weight, the 2 meters length cable section employed in the test-bench can be easily deflected. This may benefit the multirotor control in the sense that it provides a certain level of accommodation to the position deviations, but the elastic behavior of the cable and the lack of rigidity of the structure may introduce other vibration modes that tend to disturb the attitude controller.

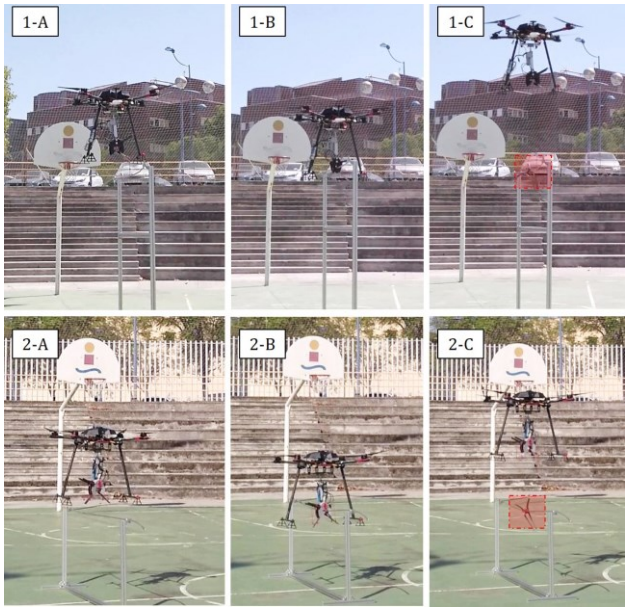

Figure 6. Sequence of images corresponding to experiments 1 and 2, showing the installation of the clip-type bird diverter.

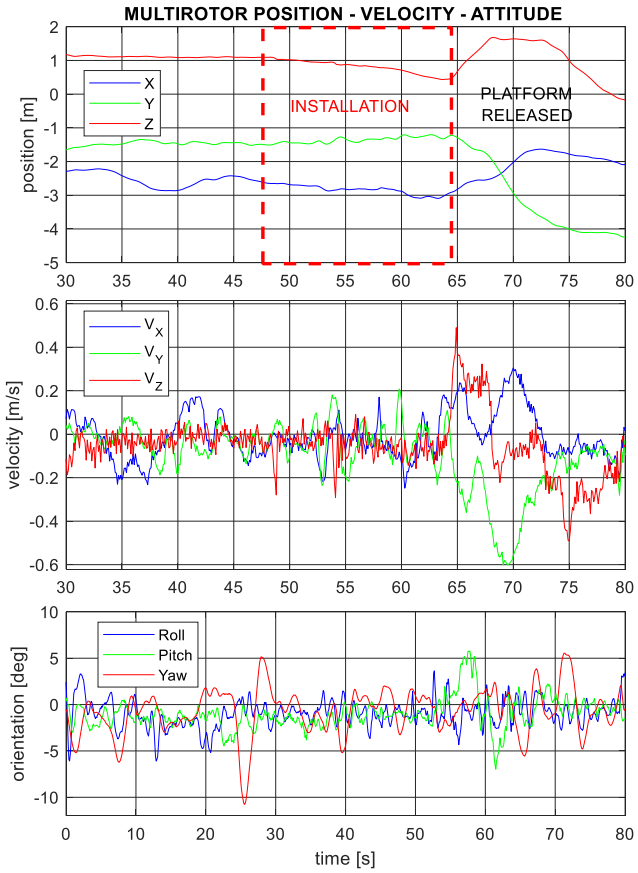

Figure 7. Multirotor position (up), velocity (middle), and attitude (down). Pink shaded area corresponds to the installation phase.

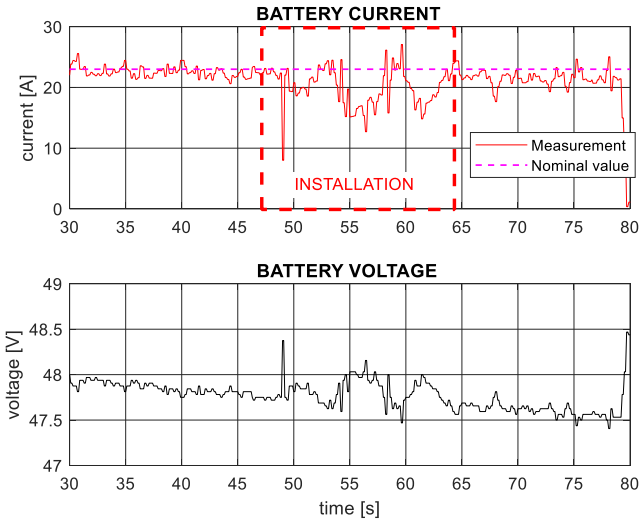

Figure 8. Multirotor battery: current (up) and voltage (down). The current drop peak at t = 49 s and around t = 55 s occurs when the platform rests on the power line supported by the installation device.

B. Electrical Interaction Test on Real Power Line

The goal of this experiment is to identify possible failures or malfunctions on the aerial platform when this approaches and interacts with the high voltage power line. Previous flight experiments [21] revealed that the electronic speed controllers may be affected by the electrostatic discharge, in such a way that the active brake protection implemented in some ESC

models may be triggered if an irregular pulse in the PWM signal is detected, causing the platform crash. The experiment is carried out in a real scenario with a 15 kV power line. In order to avoid the risk of entrapment in case the rotors stop due to the ESD, a thin aluminum rod (1 m length, 4 mm section) is attached to the installation mechanism in order to facilitate the propagation of the discharge current, while maintaining a safety distance with the power line. Figure 4 shows a sequence of images taken from the video of the experiment. The visual inspection of the video does not reveal any irregular behavior during the electrical interaction. Note that, according to [5], the minimum air insulation distance for a 15 kV power line is 5 cm. Since the installation device is electrically insulated from the multirotor control system, the probability of fault due to electrostatic discharge is reduced.

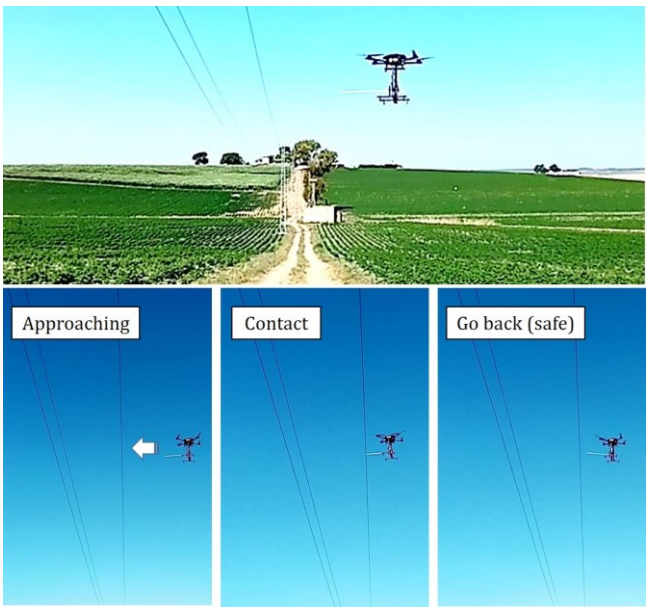

Figure 4. Sequence of images showing the contact test with a 15 kV power line, using a 1 m length aluminum rod attach to the installation mechanism.

VI. Conclusions and Future Work

This paper presented preliminary tests in a representative outdoor test-bench for validating the installation of clip-type bird flight diverters with an aerial robot equipped with a linear actuator and a clamp-like mechanism. The realization of these tests is motivated by the necessity to evaluate the reliability of the robot in the realization of this task, particularly during the installation phase when the interaction forces and wind perturbations may compromise the stability of the multirotor. Flight tests on a real 15 kV power line also evidenced that the human pilot losses the depth perception when the aerial robot is flying close to the cable, making unfeasible the realization of the installation task by manual control.

As future work, it is essential the development of a vision-based positioning system that allows the detection and localization of the power line for accurate positioning of the aerial platform.

Acknowledgment

This work is supported by the AERIAL-CORE project (H2020-2019-871479) funded by the European Commission.

References

[1] Saprem clip-type bird flight diverter specifications: https://saprem.com/balizas/salvapajaros/
[2] Crocfast clip-type bird diverters: https://birddiverter.eu/
[3] Wigeva clip-type and helical bird flight diverters: https://www.wigeva.com/productos/90
[4] Preformed helical bird flight diverter: https://preformed.com/energy/distribution/wildlife-protection/bird-flight-diverter
[5] "IEEE Guide for Maintenance Methods on Energized Power Lines," in IEEE Std 516-2009, pp.1-144, 24 June 2009.
[6] The AERIAL-CORE Project Home Page: https://aerial-core.eu/
[7] A. Ollero, M. Tognon, A. Suarez, D. Lee and A. Franchi, "Past, Present, and Future of Aerial Robotic Manipulators," in *IEEE Transactions on Robotics*, doi: 10.1109/TRO.2021.3084395.
[8] M. Orsag, C. Korpela, P. Oh, and S. Bogdan, *Aerial manipulation*, Springer Verlag, 2018.
[9] F. Ruggiero, V. Lippiello, A. Ollero, "Aerial manipulation: a literature review," in *IEEE Robotics and Automation Letters*, vol. 3, no. 3, pp. 1957-1964, July 2018.
[10] M. Á. Trujillo, *et al*, "Novel aerial manipulator for accurate and robust industrial NDT contact inspection: a new tool for the oil and gas inspection industry," in Sensors, 2019, vol. 19(6), p.1305.
[11] K. Bodie *et al*., "Active Interaction Force Control for Contact-Based Inspection with a Fully Actuated Aerial Vehicle," in *IEEE Transactions on Robotics*, vol. 37, no. 3, pp. 709-722, June 2021.
[12] P. Chermprayong, K. Zhang, F. Xiao and M. Kovac, "An integrated Delta manipulator for aerial repair: a new aerial robotic system," in *IEEE Robotics & Automation Magazine*, vol. 26(1), pp. 54-66, 2019.
[13] H. Paul, R. Miyazaki, R. Ladig, and K. Shimonomura, "TAMS: development of a multipurpose three-arm aerial manipulator system," in Advanced Robotics, vo. 35(1), pp. 31-47, 2021.
[14] A. Suarez, P. J. Sanchez-Cuevas, G. Heredia, and A. Ollero, "Aerial physical interaction in grabbing conditions with lightweight and compliant dual arms, " *Applied Sciences*, vol. 10, no. 24, p. 8927, Dec. 2020.
[15] A. Suarez, F. Real, V. M. Vega, G. Heredia, A. Rodriguez-Castaño, and A. Ollero, "Compliant bimanual aerial manipulation: standard and long reach configurations," in *IEEE Access*, vol. 8, pp. 88844-88865, 2020.
[16] H. Paul, K. Ono, R. Ladig and K. Shimonomura, "A Multirotor Platform Employing a Three-Axis Vertical Articulated Robotic Arm for Aerial Manipulation Tasks," *IEEE/ASME International Conference on Advanced Intelligent Mechatronics (AIM)*, 2018, pp. 478-485.
[17] H. W. Wopereis, T. D. van der Molen, T. H. Post, S. Stramigioli and M. Fumagalli, "Mechanism for perching on smooth surfaces using aerial impacts," *2016 IEEE International Symposium on Safety, Security, and Rescue Robotics (SSRR)*, 2016, pp. 154-159.
[18] A. Suarez, A. Caballero, A. Garofano, P. J. Sanchez-Cuevas, G. Heredia and A. Ollero, "Aerial Manipulator with Rolling Base for Inspection of Pipe Arrays," in *IEEE Access*, vol. 8, pp. 162516-162532, 2020.
[19] F. Mirallès et al., "LineDrone technology: landing an unmanned aerial vehicle on a power line," IEEE International Conference on Robotics and Automation (ICRA), Brisbane, QLD, 2018, pp. 6545-6552.
[20] N. Iversen, A. Kramberger, O. B. Schofield, and E. Ebeid, "Pneumatic mechanical systems in UAVs: autonomous power line sensor unit deployments," in IEEE International Conference on Robotics and Automation, 2021.
[21] A. Suarez, R. Salmoral, P. J. Zarco-Periñan, A. Ollero, "Experimental Evaluation of Aerial Manipulation Robot in Contact with 15 kV Power Line: Shielded and Long Reach Configurations," in IEEE Access, 2021.
[22] W. D. Greason, "Generalized model of electrostatic discharge (ESD) for bodies in approach: analyses of multiple discharges and speed of approach," in Journal of Electrostatics, vol. 54, pp. 23-37, 2002.

[23] S. Van den Berghe, D. De Zutter, "Study of ESD signal entry through coaxial cable shields," in *Journal of Electrostatics*, 1998, vol. *44*(3-4), pp. 135-148.

[24] M. Heggo, *et al*, "Operation of aerial inspections vehicles in HVDC environments Part A: Evaluation and mitigation of high electrostatic field impact," in Journal of Physics: Conference Series (vol. 1356, No. 1, p. 012009). IOP Publishing, 2019.

[25] A. Rodriguez-Castaño, S. R. Nekoo, H. Romero, R. Salmoral, J. Á. Acosta, and A. Ollero, "Installation of Clip-Type Bird Flight Diverters on High-Voltage Power Lines with Aerial Manipulation Robot: Prototype and Testbed Experimentation," *Applied Sciences*, vol. 11, no. 16, p. 7427.

[26] I. Palunko, P. Cruz and R. Fierro, "Agile load transportation: safe and efficient load manipulation with aerial robots," in *IEEE Robotics & Automation Magazine*, vol. 19, no. 3, pp. 69-79, Sept. 2012.

[27] V. Prkačin, I. Palunko and I. Petrović, "State and parameter estimation of suspended load using quadrotor onboard sensors," *International Conference on Unmanned Aircraft Systems (ICUAS)*, 2020, pp. 958-967.

[28] H. W. Wopereis, J. J. Hoekstra, T. H. Post, G. A. Folkertsma, S. Stramigioli and M. Fumagalli, "Application of substantial and sustained force to vertical surfaces using a quadrotor," *2017 IEEE International Conference on Robotics and Automation (ICRA)*, 2017, pp. 2704-2709.

[29] K. Bodie *et al*., "Active Interaction Force Control for Contact-Based Inspection With a Fully Actuated Aerial Vehicle," in *IEEE Transactions on Robotics*, vol. 37, no. 3, pp. 709-722, June 2021.

[30] Ardupilot attitude control: https://ardupilot.org/dev/docs/apmcopter-programming-attitude-control-2.html

[31] L. Meier, D. Honegger and M. Pollefeys, "PX4: A node-based multithreaded open source robotics framework for deeply embedded platforms," *2015 IEEE International Conference on Robotics and Automation (ICRA)*, 2015, pp. 6235-6240.

[32] Video of the experiments: https://youtu.be/IA6tpgcQ_Nw